JOURNAL OF CATALYSIS 68, 433–452 (1981)

In Situ Mössbauer Emission Spectroscopy Studies of Unsupported and Supported Sulfided Co–Mo Hydrodesulfurization Catalysts: Evidence for and Nature of a Co–Mo–S Phase

HENRIK TOPSØE,* BJERNE S. CLAUSEN,†,[1] ROBERTO CANDIA,* CARSTEN WIVEL,†
AND STEEN MØRUP†

** Haldor Topsøe Research Laboratories, DK-2800 Lyngby, Denmark; † Laboratory of Applied Physics II, Technical University of Denmark, DK-2800 Lyngby, Denmark*

Received June 16, 1980; revised November 25, 1980

Information regarding the structure and type of phases present in sulfided alumina-supported, as well as unsupported, Co–Mo catalysts is obtained from *in situ* Mössbauer emission spectroscopy (MES) studies. The results give the first direct evidence of the presence of a Co–Mo–S phase in alumina-supported and unsupported catalysts with similar Co/Mo ratios. Information regarding the nature of the Co–Mo–S phase is obtained from a detailed study of the Mössbauer parameters, their temperature dependence, and their sensitivity to changes in the gaseous environment. Previously proposed structural models cannot explain all the observed features of the Co–Mo–S phase. It is proposed that in alumina-supported catalysts the Co–Mo–S phase is present as single S–Mo–S slabs (i.e., one layer of the MoS_2 structure) with cobalt most likely present at molybdenum sites. For unsupported catalysts the Co–Mo–S phase consists of several slabs with bulk MoS_2-like structure. The present observations suggest that the previously observed similarities between supported and unsupported catalysts are associated with the presence of the Co–Mo–S phase in both catalyst systems. A possible reaction mechanism for hydrodesulfurization involving cobalt in the Co–Mo–S phase is proposed. Information regarding other phases in the catalysts is obtained by MES studies of Co/Al_2O_3, $CoMo_2S_4$, Co_9S_8, CoS_2, Co_3S_4, and CoS_{1+x} samples. It is observed that for a sulfided $Co–Mo/Al_2O_3$ catalyst with a composition typical of those used industrially, part of the cobalt is located in the alumina. For unsupported catalysts the effect of changing the cobalt concentration and preparation method is investigated and it is observed that under certain conditions also the thermodynamically stable cobalt sulfide, Co_9S_8, may be formed.

I. INTRODUCTION

The most commonly studied catalyst for hydrodesulfurization (HDS) or hydrotreating reactions consists of cobalt and molybdenum supported on an alumina support. The structures of both the oxidic (calcined) and the sulfided (active) states of the catalysts have been the subject of many studies. (For a review of the literature, see, e.g., (*1–4*).)

Several investigations have been directed towards an understanding of the nature and function of the cobalt promoter atoms in active $Co–Mo/Al_2O_3$ catalysts. The following three hypotheses have been widely referred to in order to describe the structure of the active catalysts:

(i) The monolayer model, proposed by Lipsch and Schuit (*5*) and Schuit and Gates (*1*), assumes that the molybdenum monolayer in the calcined catalyst remains essentially intact upon sulfiding, except for replacement of some terminal oxygen anions by sulfur anions. This model was later modified by Massoth (*6*) to account for steric effects and observed sulfur contents. The location of cobalt is somewhat uncertain, but it has been proposed that it is located inside the alumina (*1*), thereby stabilizing the monolayer.

(ii) The intercalation model, proposed by Voorhoeve and Stuiver (*7*), assumes that cobalt intercalates into the bulk of MoS_2

---

[1] Present address: Haldor Topsøe Research Laboratories, DK-2800 Lyngby, Denmark.

0021-9517/81/040433-20$02.00/0

crystals. Later Farragher and Cossee (*8*) and Farragher (*9*) proposed a modified model (the pseudointercalation model) in which intercalation is supposed to occur only at the edges of the crystals.

(iii) The contact synergy model, proposed by Delmon and co-workers (*3, 10, 11*), supposes that the active phases are present as separate phases of Co_9S_8 and MoS_2, and the promoting effect of cobalt is suggested to be the result of a contact between these phases. This model is mainly based on studies of unsupported systems, but the fact that unsupported catalysts exhibit catalytic synergy similar to that observed for supported catalysts (*12, 13*) suggests that structural and catalytic similarities may exist between unsupported and supported catalysts.

In addition to these models, others have also been presented (e.g., (*14, 15*)).

The different views on the structure of the active catalysts are probably resulting both from a great intrinsic structural complexity, which may be sensitive to the preparation parameters, and from the difficulty of experimentally studying this catalyst system, since such studies should be carried out *in situ*. This requirement is a result of the dependence of the catalyst structure on the reaction conditions (*9, 16, 17*) and in particular the necessity of avoiding exposure of the catalyst to air (*16, 18–20*). The presence of highly dispersed and noncrystalline phases may also limit the applicability of some of the techniques commonly used in studies of catalysts.

Mössbauer spectroscopy is in many respects a very suitable technique for studying the cobalt promoter atoms in the active sulfided state of Co–Mo catalysts since the applicability of this technique is not restricted by the above-mentioned complications. It is of special importance that *in situ* information can be obtained about both surface and bulk atoms in typical catalyst systems (*21*). Some of the special features of the applications of Mössbauer emission spectroscopy (MES) to Co–Mo catalysts are discussed in Section II.

We have recently applied Mössbauer spectroscopy to the study of Co–Mo and Fe–Mo catalysts supported on alumina, silica, and carbon (*16, 18, 19, 22–24*) and have found that insight into the location of the promoter atoms (Fe or Co) in the catalysts can be obtained by use of this technique. It was observed that the support not only affects the dispersion of the active phases but also influences the chemical form in which the active elements are present. Furthermore, these studies have provided, probably for the first time, direct evidence for the presence of cobalt and molybdenum in a Co–Mo–S surface phase in active $Co–Mo/Al_2O_3$ catalysts. Also for an unsupported Co–Mo catalyst containing Co in parts per million concentration, the Co–Mo–S phase was observed (*16*).

In the present paper studies on unsupported catalysts are extended to catalysts with Co/Mo ratios similar to those encountered in supported catalysts. Also the influence of the preparation method on the catalyst structure is investigated. The nature of the Co–Mo–S phase, observed in both supported and unsupported catalysts, is elucidated by detailed studies of the Mössbauer parameters of this phase. Moreover, bulk cobalt and cobalt-molybdenum sulfides, for which MES data have not been reported previously, have been investigated in order to study their possible presence in the catalysts.

In the succeeding paper (*25*) we discuss the catalytic significance of the Co–Mo–S phase by combined use of MES and catalytic activity measurements.

II. APPLICATION OF MES TO Co–Mo CATALYSTS

In view of the limited number of MES studies of catalysts and in order to avoid ambiguities in the following, some general comments on the application of this technique to Co–Mo catalysts will be given here.

It may be useful to realize that Mössbauer spectroscopy in the transmission mode can be carried out in two different ways:

(i) *Mössbauer absorption spectroscopy,* which is based on the principle that radiation from a standard radioactive source is resonantly absorbed by the Mössbauer isotope in the sample under investigation. This is by far the more commonly used mode.

(ii) *Mössbauer emission spectroscopy* (*MES*), in which the sample to be studied is doped with a radioactive isotope and used as a source. In this technique, the radiation is emitted from the sample itself and then absorbed by a standard absorber which contains the corresponding Mössbauer isotope.

Co–Mo catalysts contain no isotopes which can be used in a Mössbauer absorption experiment. However, cobalt-containing compounds can be studied by doping the compounds with ^{57}Co and using them as sources in MES experiments. Information about the cobalt atoms is then obtained by studying the ^{57}Fe atoms produced by the decay of ^{57}Co. In MES experiments the observed valence and spin states of ^{57}Fe may, however, be different from those of the parent ^{57}Co atoms. One reason for this is that iron and cobalt atoms have different chemical and electronic properties, and the stable state of Fe may therefore be different from that of Co. Secondly, the decay process itself may create unstable, but long-living ($\gtrsim 10^{-7}$ s) changes in the chemical surroundings of the Mössbauer nucleus. For a general discussion of these so-called aftereffects, see, for example, Ref. (*26*). In conducting materials the aftereffects can usually be neglected, and the observed chemical state will normally be that of iron present in low concentrations. However, the aftereffects may be quite important in insulators, and valence states different from the stable one may be observed. As an example, both Fe^{2+} and Fe^{3+} are observed in the emission spectrum of CoO (*27*) even though only Co^{2+} is present before the decay. Although the presence of aftereffects can make it difficult to obtain definite conclusions regarding the electronic state of the cobalt atoms, these effects may aid the identification of the cobalt phase present since they are sensitive to the nature of the phase. For the present investigation it is important that the immediate surroundings of the ^{57}Fe atoms are expected to be identical to those of the parent ^{57}Co atoms. Therefore, information can be obtained about the surroundings of the cobalt atoms. Moreover, the cobalt-containing phases in the catalysts can be identified by comparing the spectra of the catalysts with spectra of appropriate model compounds.

Some of the Mössbauer parameters which are particularly useful in the present study are the isomer shift, the quadrupole splitting, and the temperature dependence of the spectral area. The isomer shift, δ (the shift of the centroid of the spectrum relative to zero velocity), arises from the electrostatic interaction between the nuclear charge and the s-electron density at the nucleus. The electric quadrupole splitting, ΔE_Q (the distance between the two lines in the spectrum of a paramagnetic iron ion in noncubic symmetry), is proportional to the product of the nuclear quadrupole moment and the electric-field gradient at the nucleus. Both δ and ΔE_Q are highly sensitive to the valence and spin states (high spin or low spin) of the iron atoms. The spectral area, A, is proportional to the recoil-free fraction, f, which is given by the expression (*28*):

$$f = \exp(-k_\gamma^2 \langle x^2 \rangle), \tag{1}$$

where k_γ is the wavenumber of the γ radiation and $\langle x^2 \rangle$ is the mean square vibrational amplitude of the Mössbauer atom in the direction of the γ ray. By using the Debye model for the vibrational spectrum the following expression for the f factor in the high-temperature approximation is obtained:

$$f = \exp\left(-\frac{6E_R T}{k_B \theta_D^2}\right); \qquad T \gtrsim \theta_D/2, \tag{2}$$

where θ_D is the Debye temperature, T is the absolute temperature, E_R is the recoil energy of a free iron atom, and k_B is Boltzmann's constant. θ_D is a measure of the strength of binding of the Mössbauer atom to its surroundings.

III. EXPERIMENTAL

A. Sample Preparation

All the samples used in the MES experiments were prepared by adding radioactive, carrier-free ^{57}Co nitrate (from the Radiochemical Centre, Amersham, England) to the solutions used in the preparation. Further details are given elsewhere (*24*).

(*a*) *Model compounds.* Bulk compounds of Co_9S_8, CoS_2, Co_3S_4, and CoS_{1+x} ($0.06 \lesssim x \lesssim 0.18$) were prepared from $Co(NO_3)_2 \cdot 6H_2O$ by sulfiding in appropriate mixtures of H_2 and H_2S according to the phase diagram of the cobalt–sulfur system (e.g., (*29*)). The phase purity of the different cobalt sulfides was confirmed by X-ray powder diffraction measurements. The preparation of $CoMo_2S_4$ has been described in the literature (*30, 31*). However, the highest purity $CoMo_2S_4$ (as verified by X-ray diffraction) was obtained using the following modified process. Stoichiometric amounts of cobalt formate (doped with radioactive ^{57}Co) were first added to finely powdered MoS_2. This mixture was then pressed into a pellet, placed in a quartz ampoule, and heated up to 575 K in a H_2 flow and kept at this temperature for 3 h in order to decompose the cobalt formate. After cooling to room temperature, the ampoule was evacuated to about 0.1 Pa and then sealed. Finally, the ampoule was heated progressively for a period of 6 h up to 1175 K and was kept at this temperature for 16 h before it was allowed to cool slowly to room temperature.

(*b*) *Unsupported catalysts.* Two unsupported catalysts were prepared by impregnation of MoS_2 powder (Riedel-de Haën AG; BET surface area = 1.79 m^2g^{-1}; crystallite dimension obtained from the X-ray (002) reflection: $D^{002} \sim 65$ nm) with aqueous solutions of cobalt nitrate. One of these catalysts, which has briefly been discussed previously (*16*), has an atomic Co/Mo ratio of about 3×10^{-6}. This sample is denoted Co/MoS_2(ppm). The other sample has a ratio of Co/Mo = 0.05 and is denoted Co/MoS_2(0.05). The impregnation step was in both cases followed by treatment in H_2/H_2S (2% H_2S) at around 600 K for at least 4 h.

A third unsupported catalyst was prepared by adding simultaneously, under vigorous stirring, solutions of ammonium heptamolybdate and cobalt nitrate to a solution of ammonium sulfide. The solutions were kept at 350 K. After evaporation to dryness at 350 K the resulting product was treated in H_2S/H_2 (6% H_2S) at 600 K for 4 h. This catalyst, which has a Co/Mo atomic ratio of 0.25, is denoted Co/MoS_2(0.25).

(*c*) *Supported catalysts.* The Co/Al_2O_3 catalyst contained 0.25% (by weight) Co and was prepared by impregnation of η-Al_2O_3 (230 m^2g^{-1}) with cobalt nitrate. The $Co–Mo/Al_2O_3$ catalyst containing 1% Co and 6% Mo (corresponding to a Co/Mo atomic ratio of 0.27) was prepared by coimpregnation of the alumina with an ammoniacal solution of cobalt nitrate and ammonium heptamolybdate. The impregnated samples were dried in air at room temperature and calcined in air for 24 h at 775 K. The samples were then sulfided at 600 K in H_2/H_2S (2% H_2S) for at least 24 h prior to collection of the Mössbauer spectra.

B. Mössbauer Spectroscopy Measurements

In the present MES measurements the catalysts and the model compounds are used as stationary sources. The energy spectra of the emitted γ rays from the sources were measured by absorption in a moving single-line absorber of $K_4Fe(CN)_6 \cdot 3H_2O$ (obtained from New England Nuclear). The potassium ferrocyanide, enriched in ^{57}Fe to more than 90%, was embedded in a Lucite matrix and contained 0.25 mg ^{57}Fe/cm^2. The constant-acceleration Mössbauer spectrometer was calibrated using a source of ^{57}Co in metallic iron. Zero velocity is defined as the centroid of the calibration spectrum obtained at room temperature. Positive velocities correspond to the absorber moving away from the source. Thus, the isomer shifts are directly comparable to those obtained in absorption experiments. The linewidth of the calibration spectra was 0.28 ± 0.01 mm s^{-1}.

The samples were doped with ^{57}Co in an amount corresponding to an activity of about 40 MBq (3.7 × 10^{10} Bq = 1 Ci) and a reasonable signal-to-noise ratio was achieved by using counting times in excess of 24 h for each spectrum. This results in about 10^6 counts in each of the 256 channels in the folded spectra.

The catalyst samples were pressed into thin self-supporting wafers with a diameter of 12.5 mm and placed in the *in situ* cell shown in Fig. 1. This cell was used for measurements at and above room temperature and was constructed of Pyrex glass. The γ radiation is transmitted through a window in the Pyrex cell, blown to a thickness of about 0.1 mm. With this thickness, the intensity of the 14.4-keV γ radiation is only reduced by about 15%. The cell has two windows, thus also allowing absorption studies to be carried out. The sample wafers are placed in a stainless-steel holder and are kept in place by a thread ring. The holder is fixed in position in the cell by springs. Temperature measurements are carried out by means of a thermocouple located about 5 mm below the sample. A temperature stability better than ±3 K was obtained by use of an electronic regulating system. The real sample temperature was slightly different from the measured one. Corrections for this difference were made separately (*19*) by use of thermocouples embedded in a pressed wafer of alumina which replaced the sample in this experiment.

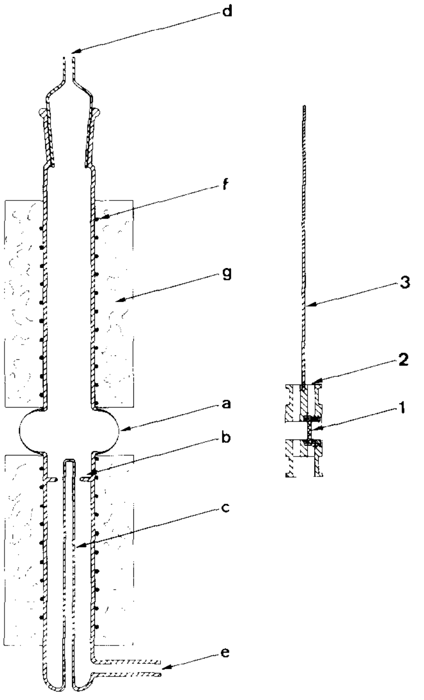

FIG. 1. *In situ* cell for emission Mössbauer spectroscopy studies. (a) Window for transmission of γ rays; (b) basis for absorber holder; (c) tube for temperature measurement and regulation; (d) inlet of gas; (e) outlet of gas; (f) heating coil; (g) insulating material; (1) catalyst; (2) channels for gas flow; (3) rod for removal of the absorber holder.

Measurements on catalysts below room temperature were carried out in a cell (*19*) which could be sealed at reaction conditions and subsequently transferred to a low-temperature cryostat.

The spectra were computer-fitted with a number of Lorentzian lines using a Fortran program written by Sørensen (*32*). This program employs a least-squares procedure with "random walk" iterations and allows the use of constraints. The uncertainties in the Mössbauer parameters given in the tables were estimated from a number of fits in which different constraints were applied to the line parameters.

IV. RESULTS

Figure 2 shows MES spectra of the model compounds Co_9S_8, CoS_2, Co_3S_4, CoS_{1+x}, and $CoMo_2S_4$ obtained at room

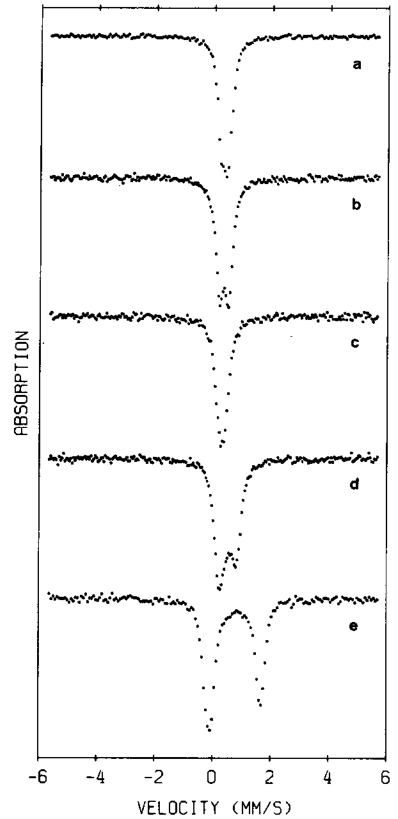

FIG. 2. Room-temperature Mössbauer spectra of model compounds. (a) Co_9S_8; (b) CoS_2; (c) Co_3S_4; (d) CoS_{1+x}; and (e) $CoMo_2S_4$.

temperature. Figure 3 shows room-temperature spectra of the unsupported catalysts Co/MoS_2(ppm), Co/MoS_2(0.05), and Co/MoS_2(0.25), whereas spectra of the Co/Al_2O_3 and the $Co–Mo/Al_2O_3$ catalysts are shown in Fig. 4. The corresponding Mössbauer parameters obtained from computer fits of the spectra are given in Tables 1 and 2. The temperature dependences of the spectral areas for Co_9S_8, $CoMo_2S_4$, Co/MoS_2(ppm), and $Co–Mo/Al_2O_3$ are shown in Fig. 5. The Debye temperatures, θ_D, estimated from the high-temperature section of the curves are indicated in the figure. It is found that the low-temperature experimental data for the Co/MoS_2(ppm) and the $Co–Mo/Al_2O_3$ catalysts cannot be fitted with the Debye model, and the model is used only in order to obtain a measure for the temperature dependence of the spectral area. The Debye temperatures for the other model compounds were all found to be similar to the values for Co_9S_8 and $CoMo_2S_4$. The temperature dependences of the isomer shifts and the quadrupole splittings are shown in Fig. 6 and Fig. 7, respectively.

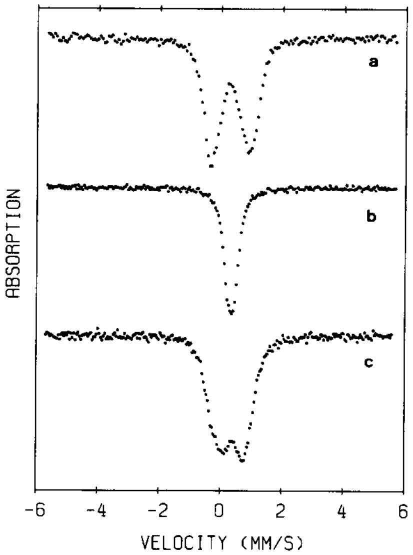

FIG. 3. Room-temperature Mössbauer spectra of unsupported catalysts. (a) Co/MoS_2(ppm); (b) Co/MoS_2(0.05); and (c) Co/MoS_2(0.25).

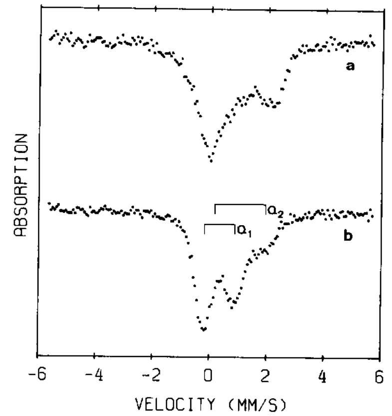

FIG. 4. Mössbauer spectra of the alumina-supported catalysts at room temperature. (a) Co/Al_2O_3; this spectrum was obtained after calcination. (b) $Co–Mo/Al_2O_3$; the spectrum was obtained in a gas mixture of H_2S/H_2 (2% H_2S).

TABLE 1

Room-Temperature Mössbauer Parameters for Model Compounds

Compound	Doublet (1)[a]		Doublet (2)[a]		Single line[a]
	$\delta(1)$ (mm s^{-1})	$\Delta E_Q(1)$ (mm s^{-1})	$\delta(2)$ (mm s^{-1})	$\Delta E_Q(2)$ (mm s^{-1})	δ (mm s^{-1})
Co_9S_8	0.35 ± 0.01	0.26 ± 0.01			0.37 ± 0.01
CoS_2	0.36 ± 0.01	0.32 ± 0.01			
Co_3S_4					
(i)	0.30 ± 0.01	0.18 ± 0.01			
(ii)					0.30 ± 0.01
CoS_{1+x}					
(i)	0.48 ± 0.01	0.29 ± 0.01	0.51 ± 0.01	0.67 ± 0.01	
(ii)	0.51 ± 0.01	0.61 ± 0.01			0.44 ± 0.01
$CoMo_2S_4$	0.07 ± 0.02	0.66 ± 0.02	0.81 ± 0.01	1.74 ± 0.01	

Note. (i) and (ii) represent two possible fits of the same spectrum.

[a] The isomer shift and quadrupole splitting are δ and ΔE_Q, respectively.

A. Model Compounds

MES results of the model compounds Co_9S_8, CoS_2, Co_3S_4, CoS_{1+x}, and $CoMo_2S_4$ are described in detail in the present paper in order to establish their possible presence in the sulfided catalysts. Co_9S_8, which is the thermodynamically stable cobalt sulfide under typical reaction conditions, has been proposed to be present in sulfided Co–Mo catalysts (see, e.g., Refs. (*10–12*, *33*)). The cobalt sulfides, CoS_2, Co_3S_4, and CoS_{1+x} have not been reported to be present in active catalysts, but have been observed in unsupported Co–Mo catalysts after certain sulfiding procedures (*10*, *34*). The presence of $CoMo_2S_4$ in sulfided catalysts was proposed by Lo Jacono *et al.* (*35*). Although $CoMo_2S_4$ was found to be catalytically inactive by Hagenbach *et al.* (*12*), it may of course still be present in the catalyst.

The spectrum of Co_9S_8 (Fig. 2a) consists of three overlapping lines, a quadrupole doublet due to cobalt in tetrahedral sites, and a single line due to cobalt in octahedral sites (*36*). The isomer shift and quadrupole

TABLE 2

Room-Temperature Mössbauer Parameters for Unsupported and Supported Catalysts

Catalyst	Doublet (1)[a]		Doublet (2)		Single line
	$\delta(1)$ (mm s^{-1})	$\Delta E_Q(1)$ (mm s^{-1})	$\delta(2)$ (mm s^{-1})	$\Delta E_Q(2)$ (mm s^{-1})	δ (mm s^{-1})
Unsupported catalysts					
Co/MoS_2(ppm)	0.32 ± 0.03	1.21 ± 0.03			
Co/MoS_2(0.05)			0.36 ± 0.02	0.22 ± 0.02	0.35 ± 0.02
Co/MoS_2(0.25)[b]	0.34 ± 0.05	1.03 ± 0.05	0.35	0.26	0.37
Supported catalyst					
Co–Mo/Al_2O_3[c]	0.33 ± 0.05	1.05 ± 0.05	1.06 ± 0.07	1.78 ± 0.07	

[a] Doublet (1) is the spectral component due to the Co–Mo–S phase.

[b] This spectrum was fitted using five lines, two of which were unconstrained, and three (Doublet (2) and Single line) of which were constrained to the position and area ratio found in the spectrum of bulk Co_9S_8.

[c] Doublet (1) and Doublet (2) correspond to Q_1 and Q_2, respectively, in Fig. 4b.

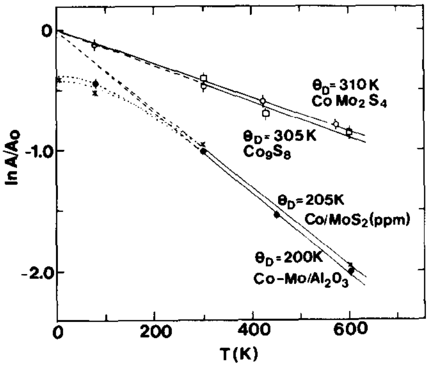

FIG. 5. Temperature dependence of the Mössbauer spectral area, A. The area, A_0, is obtained by extrapolating the straight-line data obtained at high temperature to T = 0 K. The results for Co–Mo/Al_2O_3 refer to the Q_1 component.

splitting values of Co_9S_8, shown in Figs. 6 and 7, are those of the quadrupole doublet component. The value of the quadrupole splitting is quite small at all temperatures. Therefore, the spectrum of Co_9S_8 can essentially be described as a relatively narrow single line. The area ratio of the quadrupole doublet to the single-line component is about 8 : 1, which is in accordance with the 32 : 4 site occupancy of tetrahedral to octahedral metal sites of Co_9S_8 in the unit cell (*37*). Magnetic susceptibility measurements (*38*) have shown that Co_9S_8 is a Pauli paramagnet down to 4.2 K behaving like a metal with no resultant magnetic moments on the metal atoms. Our Mössbauer results on ^{57}Co-doped Co_9S_8, which showed no magnetic ordering down to 5.8 K, are in agreement with these observations. A Debye temperature of θ_D = 305 ± 30 K was obtained from the plot in Fig. 5.

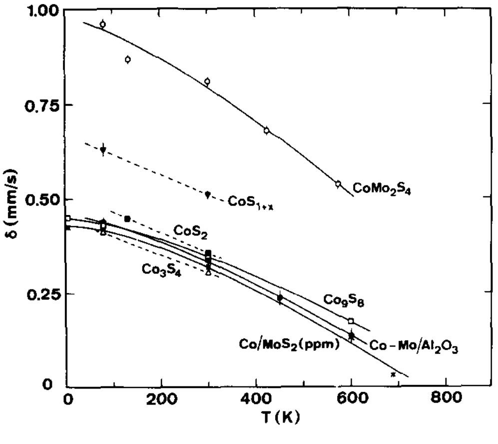

FIG. 6. The isomer shift, δ, plotted against the temperature, T, for model compounds and catalysts. The results for Co–Mo/Al_2O_3 refer to the Q_1 component.

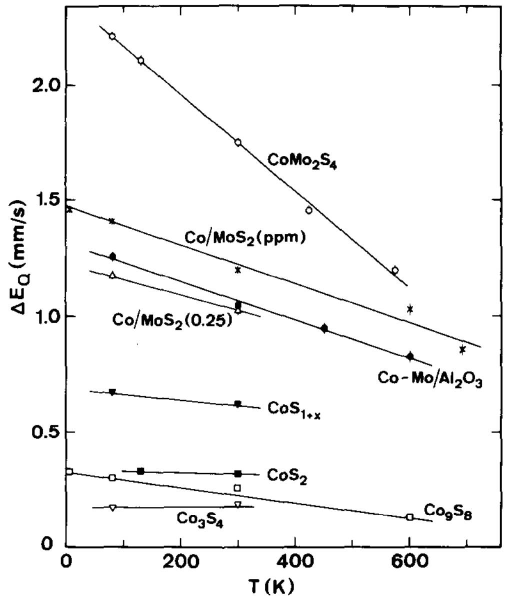

FIG. 7. Temperature dependence of the quadrupole splitting, ΔE_Q, for model compounds and catalysts. The results for Co–Mo/Al_2O_3 refer to the Q_1 component.

CoS_2, which has the pyrite structure with the cobalt atoms octahedrally surrounded by sulfur (*39*), is a ferromagnetic metallic conductor with a Curie temperature of about 120 K (*40*). The room-temperature Mössbauer spectrum of this compound (Fig. 2b) shows a single quadrupole doublet with quadrupole splitting and isomer shift values given in Table 1. The quadrupole doublet persists down to the transition temperature, whereas at lower temperatures a broad absorption pattern is observed. The observation that the quadrupole splitting is almost constant over the temperature range from 130 to 300 K (Fig. 7), and the fact that magnetic splitting is so small that it is not resolved in the low-temperature spectra suggest that the iron atoms after the decay are present as low-spin Fe^{2+}. Thus, in this compound, the valence state and the spin state of the parent atoms seem to be the same as those of the daughter atoms. Mössbauer absorption results of ^{57}Fe-doped CoS_2 ($Co_{0.99}Fe_{0.01}S_2$) (*41*) gave spectra identical to those reported here of ^{57}Co-doped CoS_2. This shows that aftereffects are not important in this compound.

Co_3S_4 has the spinel structure (*42*) and is a weakly paramagnetic, metallic conductor (*43*). At room temperature only a single broad absorption line is observed (Fig. 2c). This component can be interpreted as (i) a quadrupole doublet with a small and nonresolved splitting or (ii) a broad single line. Both interpretations are included in Table 1. The value of the quadrupole splitting shown in Fig. 7 is the one obtained from analysis (i). At 80 K a line appears at around 0 mm s^{-1} and this line can be interpreted as the low-velocity line in a quadrupole doublet. This new component is believed to be due to aftereffects following the decay of ^{57}Co.

CoS_{1+x} ($0.06 \leq x \leq 0.18$), which has the NiAs structure with the cobalt atoms octahedrally surrounded by sulfur (*44*), has been found to be a Pauli-paramagnetic, metallic conductor (*45*). At room temperature, the Mössbauer spectrum of CoS_{1+x} (Fig. 2d) shows an asymmetric two-line pattern which can be interpreted as consisting of a quadrupole doublet and a single line or as two quadrupole doublets (Table 1). The spectrum at 80 K is similar to that obtained at room temperature except for a more pronounced asymmetry. The presence of more than one component in the spectra suggests that cobalt is located in several types of sites. This is in accordance with the nonstoichiometry of the CoS_{1+x} phase resulting in cobalt sites with different surroundings. It is interesting that the isomer shifts of both components fall between those of low-spin Fe^{3+} and high-spin Fe^{2+}.

$CoMo_2S_4$ has been found by Van den Berg (*30*) and Anzenhofer and de Boer (*46*) to have a monoclinic crystal structure in which Co, as well as Mo, occupies distorted octahedral positions. Figure 2e shows a spectrum of $CoMo_2S_4$ at room temperature. The predominant part of the spectrum consists of a quadrupole doublet with an isomer shift typical of high-spin Fe^{2+} (Table 1). In addition to the high-spin Fe^{2+} component, a second quadrupole doublet, which can be assigned either to low-spin Fe^{2+} or to high-spin Fe^{3+}, is also observed in the spectrum. The relative intensity of this latter component is observed to increase with decreasing temperature. This suggests a high-spin to low-spin transition or a temperature dependence of aftereffects. High-spin to low-spin transitions have been observed in other sulfides (e.g., (*47*)). The values of the isomer shift and quadrupole splitting plotted in Figs. 6 and 7 are those of the high-spin ferrous component. From magnetic measurements on $CoMo_2S_4$ (*30*) it has been concluded that Co is present as low-spin Co^{2+}. The present Mössbauer results therefore suggest that the parent and daughter atoms in $CoMo_2S_4$ have the same valence state above room temperature, whereas at lower temperature also the spin states seem to be the same. The temperature dependence of the total spectral area of $CoMo_2S_4$ is plotted in Fig. 5. A Debye temperature of $\theta_D = 310 \pm 20$ K is obtained.

B. Unsupported Catalysts

The spectrum of the cobalt-doped MoS_2, Co/MoS_2(ppm), (Fig. 3a), shows a two-line pattern with parameters very different from those of the cobalt sulfides and the $CoMo_2S_4$ compound. The isomer shift is in accordance with either Fe^{2+} in the low-spin state, Fe^{3+} in the high-spin state, or Fe^{3+} in the low-spin state. However, as shown in Fig. 7, the quadrupole splitting of the spectrum decreases by about 40% when the temperature is raised from 3.4 to 693 K. This is consistent only with Fe^{3+} in the low-spin state, since low-spin Fe^{2+} and high-spin Fe^{3+} have quadrupole splittings which are independent of temperature. It is noteworthy that the isomer shift is larger than the values normally found in low-spin Fe^{3+} compounds. The isomer shifts of Fe^{2+} and Fe^{3+} low-spin compounds are quite similar and, for example, in the case of low-spin iron cyanides, values close to 0 mm s^{-1} are usually reported (*48*). However, the isomer shifts depend upon the type of ligands and, for example, in Fe^{2+} low-spin sulfides, shifts up to 0.38 mm s^{-1} (at 300 K) have been found (*49*), and since the cobalt atoms in the Co/MoS_2(ppm) catalyst have sulfur ligands the observed isomer shift (0.32 mm s^{-1} at 300 K) is in agreement with the Fe^{3+} low-spin assignment. A relatively low Debye temperature for the Co/MoS_2(ppm) catalyst ($\theta_D = 205 \pm 10$ K) is obtained from the plot of the total spectral area in Fig. 5. This Debye temperature is significantly lower than the values obtained for the model compounds discussed above.

In the spectrum of the Co/MoS_2(0.05) catalyst (Fig. 3b), prepared in the same way as the Co/MoS_2(ppm) catalyst, Co_9S_8 is the only cobalt phase that can be detected. However, other cobalt phases could be present in low concentration ($\lesssim 5\%$) without being observed in the Mössbauer spectra.

The unsupported catalyst prepared by coprecipitation, Co/MoS_2(0.25), shows a Mössbauer spectrum (Fig. 3c) that is quite different from that of Co/MoS_2(0.05) (Fig. 3b). The spectrum can be analysed in terms of two components (see Table 2): one, a doublet which is similar to that observed in the Co/MoS_2(ppm) catalyst, but with a slightly smaller quadrupole splitting, and one which can be identified as Co_9S_8. The quadrupole splitting values of Co/MoS_2(0.25) in Fig. 7 are those of the quadrupole doublet. The temperature dependence of the area of this component (Fig. 5) is identical to that of the Co/MoS_2(ppm) catalyst. A computer analysis of the spectra of Co/MoS_2(0.25), taking into account the different f factors for the two components, shows that about 80% of the cobalt atoms are present in a phase similar to that observed for the Co/MoS_2(ppm) catalyst. X-Ray powder diffraction measurements of the Co/MoS_2(0.25) catalyst showed a diagram very similar to that of "rag-type" MoS_2 obtained by Chianelli *et al.* (*50*) except for different relative intensities of the diffraction lines. Thus, a poorly crystallized MoS_2-like structure has formed, and a crystallite size of $D^{002} = 3.5$–4.0 nm was estimated from the width of the (002) diffraction line. Apart from this phase, no lines from a separate cobalt sulfide or any other phase could be observed in the diffraction diagram.

It is noteworthy that exposure of the unsupported catalysts to air at room temperature did not give rise to any changes in the Mössbauer spectra, whereas the spectra of alumina-supported catalysts were significantly affected by this treatment (*16*).

C. Alumina-Supported Catalysts

The MES spectrum of the calcined Co/Al_2O_3 catalyst (Fig. 4a) shows that two iron species are present. The main doublet has a quadrupole splitting $\Delta E_Q = 2.13 \pm 0.05$ mm s^{-1} and an isomer shift $\delta = 1.09 \pm 0.05$ mm s^{-1}. This is typical of high-spin Fe^{2+}. The other component ($\Delta E_Q = 1.08 \pm 0.07$ mm s^{-1} and $\delta = 0.39 \pm 0.07$ mm s^{-1}) can be assigned to a high-spin ferric component.

Figure 4b shows a spectrum of the Co–Mo/Al_2O_3 catalyst at 300 K after sulfiding at 600 K. As indicated by the bar diagram, the spectrum can be analysed in terms of two quadrupole doublets (Q_1 and Q_2), which shows that cobalt in the sulfided catalyst is present at two different sites. The absorption lines for Q_1 and Q_2 are much broader than the natural linewidth, reflecting a distribution in the Mössbauer parameters. The large isomer shift and the temperature-dependent quadrupole splitting observed for Q_2 are typical of high-spin Fe^{2+}. The parameters of this component are quite similar to those for the high-spin Fe^{2+}

component in the Co/Al_2O_3 sample. The values for the Mössbauer parameters for Q_1 and the temperature dependence of these parameters (Figs. 6 and 7) are very similar to those observed for the unsupported Co/MoS_2(ppm) and Co/MoS_2(0.25) catalysts. The temperature dependence of the spectral area of Q_1 is plotted in Fig. 5, and from the straight-line section of the curve a Debye temperature of $\theta_D = 200 \pm 10$ K can be estimated. This is also similar to the values of θ_D for the Co/MoS_2(ppm) and Co/MoS_2(0.25) catalysts. In addition to the components Q_1 and Q_2, the spectrum of the $Co–Mo/Al_2O_3$ catalyst may also contain a low-intensity Fe^{3+} (high-spin) component similar to that observed in the Co/Al_2O_3 sample.

V. DISCUSSION

For paramagnetic compounds such as those discussed in this paper, the isomer shift and the quadrupole splitting depend mainly on the local surroundings of the Mössbauer isotope. Therefore, the spectra are essentially independent of particle size (*21*). Consequently, the spectra of the catalysts can be compared with those of well-crystallized model compounds in order to identify the nature of the phases which are present in the catalysts, even if these phases have such small dimensions or are so poorly crystallized that detection by X-ray diffraction is not possible.

A. UNSUPPORTED Co–Mo CATALYSTS

The study of unsupported catalysts is interesting from the point of view that such catalysts show a behavior similar to that of supported catalysts with respect to the strong positive catalytic synergy exhibited by the active metals, i.e., the activity of catalysts containing both metals is greater than that expected from the individual component catalysts. A maximum in activity for supported as well as unsupported catalysts is usually obtained for Co/Mo ~ 0.4 – 1.0 [Co/(Co + Mo) ~ 0.3 – 0.5]. These results suggest that structural and catalytic similarities may exist between unsupported and supported catalysts. Consequently, several investigators (*7, 8, 10–14, 33*) have used the approach of studying unsupported catalysts in order to obtain information about the more elusive supported catalysts.

The Co/MoS_2(ppm) unsupported catalyst has a Mössbauer spectrum which differs from those of the cobalt sulfides and $CoMo_2S_4$. Consequently, the presence of cobalt in any significant amount in such phases can be ruled out. This result also shows that the immediate surroundings of the cobalt atoms are different from those of cobalt in the model compounds. Thus, the cobalt atoms in the Co/MoS_2(ppm) catalyst seem to be intimately associated with the MoS_2 structure. This cobalt-containing phase is for convenience denoted Co–Mo–S. As discussed in Section IV.B, the values of the Mössbauer parameters and their temperature dependence show that in this phase the Fe^{3+} atoms, produced by the decay of cobalt, have a low-spin electronic configuration. This is a strong indication that the Fe atoms (and thus the parent Co atoms) have sulfur surroundings, since oxygen surroundings generally result in a high-spin configuration. This result is not unexpected since the pretreatment of the sample should ensure the absence of significant amounts of oxygen.

Hagenbach *et al.* (*10*) observed by X-ray diffraction studies on a series of unsupported catalysts and anomalously low MoS_2 *c* parameter for a sample with a low cobalt concentration (Co/(Co + Mo) = 0.01). This finding was interpreted as cobalt being associated with the MoS_2 lattice. However, for higher cobalt contents, these authors observed the normal *c* parameter and the presence of a separate Co_9S_8 phase. It has therefore been suggested by Delmon (*33*) that our previous observation (*16*) of the Co–Mo–S phase in an unsupported catalyst (the Co/MoS_2(ppm) catalyst) is due to the fact that cobalt is present in very small amounts. The results on the Co/MoS_2(0.05) catalyst, which was prepared in the same way as the Co/MoS_2(ppm) catalyst, could seem to be in accordance with this suggestion since only Co_9S_8 is observed in the spectrum of the Co/MoS_2(0.05) catalyst (Fig. 3b). Thus, from the experiments on the Co/MoS_2(ppm) and the Co/MoS_2(0.05) catalysts alone, one might indeed conclude that the Co–Mo–S phase is important only for catalysts with low Co/Mo ratios.

The results on the Co/MoS_2(0.25) catalyst are, however, inconsistent with the above conclusion. This catalyst has a higher Co/Mo ratio than the Co/MoS_2(0.05) catalyst, but nevertheless the Mössbauer spectra show that most of the cobalt atoms are present in the Co–Mo–S phase. These results therefore clearly demonstrate that the Co–Mo–S phase may also be encountered in unsupported catalysts with Co/Mo ratios in the range where maximum catalytic activity occurs. Furthermore, the results on the Co/MoS_2(0.25) catalyst show that quite large amounts of cobalt can be accommodated in the Co–Mo–S phase. From the analysis of the relative spectral areas it can be estimated that the Co/Mo ratio in this phase is not less than ~0.2. The value of 0.2 is obtained if all the molybdenum atoms in the catalyst are present in the Co–Mo–S phase.

The fact that the Co–Mo–S phase is the predominant cobalt phase in the catalyst with the high Co/Mo ratio (Co/MoS_2(0.25)) but not in the catalyst with the lower Co/Mo ratio (Co/MoS_2(0.05)) is undoubtedly related to differences in the preparation procedures. The Co/MoS_2(0.05) catalyst was prepared by impregnation of MoS_2, whereas the Co/MoS_2(0.25) catalyst was prepared by coprecipitation. Thus, the formation of the Co–Mo–S phase seems to be favored by an intimate contact between cobalt and molybdenum during the preparation. If such a contact does not exist, nucleation of the thermodynamically stable cobalt sulfide (Co_9S_8 in the present case) may dominate. The results for the Co/MoS_2(ppm) and Co/MoS_2(0.05) catalysts, both prepared by impregnation, show that the formation of Co_9S_8 can also be suppressed by lowering the cobalt concentration.

It is interesting that several previous investigators (see, e.g., (*33*)) have observed that an "intimate contact" during the preparation of unsupported catalysts results in increased catalytic activity. In view of the present results this observation seems to suggest that the catalytic activity is associated with the Co–Mo–S phase and not with Co_9S_8. This is further supported by the results given in Ref. (*25*).

At present, the exact role of different preparation parameters (e.g., crystallinity and surface area of MoS_2, nature of precursor phases, mixing degree of phases, and sulfiding conditions) leading to the genesis of the Co–Mo–S phase is not completely understood and still needs further study.

The Mössbauer parameters of the Co–Mo–S phase in the Co/MoS_2(0.25) catalyst are very similar to those observed for the Co/MoS_2(ppm) catalyst (see Figs. 5–7). It is, however, interesting to note that the quadrupole splitting for the Co/MoS_2(0.25) catalyst is slightly smaller (about 0.15 mm s^{-1} at all temperatures) than the splitting observed for the Co/MoS_2(ppm) catalyst. This result is not surprising in view of the likelihood that the Co–Mo–S phase has very different compositions (Co/Mo ratios) for the two catalysts. Consequently, different local surroundings are expected for the cobalt atoms in the two catalysts. Moreover, the difference in crystallite dimension between the two catalysts may also give rise to minor differences in the quadrupole splittings (*21*).

Although Mössbauer spectroscopy showed that large amounts of the Co–Mo–S phase are present in the Co/MoS_2(0.25) catalyst, X-ray diffraction measurements only showed the presence of a MoS_2-like phase. This either means that the Co–Mo–S phase is X-ray amorphous or that the structure of the Co–Mo–S phase is similar to that of MoS_2. However, the fact that the Co–Mo–S phase is observed in the MES spectra of the Co/MoS_2(ppm) catalyst, prepared by impregnation of well-crystallized MoS_2, favors the latter possibility. The location of Co in the Co–Mo–S phase is discussed further in Sections V.B.b.2 and V.C.

B. ALUMINA-SUPPORTED CATALYSTS

The present Mössbauer spectroscopy investigations are mainly concerned with the presence of the Co–Mo–S phase in sulfided catalysts. There may, however, also exist other cobalt-containing phases in such catalysts, depending on content of active metals, preparation method, type and surface area of the support, calcination conditions, etc. Apart from cobalt in the Co–Mo–S phase, cobalt may also be present in alumina, as discussed below, or in cobalt phases like Co_9S_8. This latter phase may be found, for example, in catalysts having high Co/Mo ratios (*25*).

(*a*) *Co/Al$_2$O$_3$*

It has been proposed that, upon sulfiding a Co–Mo/Al_2O_3 catalyst, cobalt may remain completely (*1, 2, 50*) or partly (*51–53*) inside the alumina. In view of this we have included the spectrum of the calcined Co/Al_2O_3 sample where all the cobalt was shown (*24*) to be located in the alumina lattice. The spectrum shows a broad high-spin Fe^{2+} doublet, most likely arising from Co^{2+} located in sites with different local surroundings in the alumina lattice. In addition to this doublet a high-spin Fe^{3+} component is also present. This component may, for example, originate from the presence of Co^{3+} before the decay or may be due to aftereffects (see Section II).

(*b*) *Sulfided Co–Mo/Al$_2$O$_3$*

(*1*) *Presence of cobalt in alumina.* The Mössbauer spectrum of the sulfided Co–Mo/Al_2O_3 catalyst (Fig. 4b) shows that cobalt is present in two main configurations. One of these, giving rise to the quadrupole doublet, Q_2, can be assigned to cobalt located in the alumina since this component was also observed in the Co/Al_2O_3 sample. The linewidth of this component is, as was also the case for the Co/Al_2O_3 catalyst, significantly larger than the natural linewidth indicating that the cobalt atoms are not forming a well-defined phase such as, for example, $CoAl_2O_4$. Rather the cobalt atoms are present in sites of slightly different symmetry. From the relative spectral area of the Q_2 doublet it is estimated that about 30% of the cobalt atoms are located in the alumina after sulfiding of the Co–Mo/Al_2O_3 catalyst. This shows that a significant amount of the cobalt atoms is unaffected by the sulfiding treatment. The amount of cobalt located in the alumina lattice may depend on the details of the preparation and sulfiding procedures.

(*2*) *Characteristics of the Co–Mo–S phase.* Apart from cobalt located in the alumina, cobalt atoms are present in a phase which gives rise to the quadrupole doublet, Q_1. This doublet is not observed in any of the spectra of the cobalt sulfides or $CoMo_2S_4$, but is observed for the Co/MoS_2(ppm) and Co/MoS_2(0.25) unsupported catalysts (see Section V.A.). The Q_1 doublet therefore originates from the Co–Mo–S phase. This phase was also observed for Co–Mo catalysts supported on silica and carbon (*22, 24*). In the following, the Mössbauer results will be discussed with the aim of characterizing the chemical composition and structure of the Co–Mo–S phase.

The present Co–Mo catalyst is alumina supported and it is interesting to consider if the Co–Mo–S phase may contain aluminum or oxygen. These elements might be present as a result of, for example, interdiffusion or incomplete sulfiding. The Mössbauer results suggest that these elements cannot be present to any appreciable extent in the Co–Mo–S phase. First of all, the similarity between unsupported and supported catalysts indicates that no elements other than Co, Mo, and S are present in the Co–Mo–S phase. Secondly, it is observed that the iron atoms, produced by the decay of Co, are present in the low-spin Fe^{3+} state, a spin state which would not be expected if the cobalt atoms were bonded to oxygen atoms.

The approximate chemical composition of the Co–Mo–S phase can be estimated from the Mössbauer results. From the analysis of the spectra of the Co–Mo/Al_2O_3 catalyst it is found that about 70% of the cobalt atoms are located in the Co–Mo–S phase, corresponding to a Co/Mo ratio of 0.2 assuming that all the molybdenum atoms in the catalyst are present in this phase. This ratio will of course be higher if part of the molybdenum is present in other phases. The results presented in Ref. (*25*) suggest that even higher amounts of cobalt can be accommodated in the Co–Mo–S phase. It should be noted that the Co–Mo–S phase may have a broad range of compositions. In Section V.A it was discussed that the value of the quadrupole splitting for the Co–Mo–S phase seems to be a function of the Co/Mo ratio in this phase. The Q_1 doublet for the Co–Mo/Al_2O_3 catalyst has a quadrupole splitting quite similar to that of the Co–Mo–S phase in the unsupported Co/MoS_2(0.25) catalyst, which is consistent with the observation that the Co–Mo–S phases in the two catalysts have similar compositions.

Previous MES results have given information regarding the dispersion of Co in the Co–Mo–S phase. Exposure of the sulfided Co–Mo/Al_2O_3 catalyst to air at room temperature changed the state of the iron atoms, produced by the decay of the cobalt atoms in the Co–Mo–S phase (*16*). Also, the valence state of the cobalt promoter atoms in the Co–Mo–S phase was found to be sensitive to changes in the reaction gas mixture. These results show that the different gas molecules have easy access to the cobalt atoms, revealing that most of these atoms are located at the surface of the Co–Mo–S phase. Furthermore, the fact that a large fraction of the atoms in this phase are cobalt atoms leads us to the conclusion that, in the case of the alumina-supported catalyst, the entire Co–Mo–S phase must be highly dispersed. The observation of a linear relation between the catalytic activity and the amount of the Co–Mo–S phase (*25*) also indicates a high state of dispersion of the Co–Mo–S phase.

With respect to the genesis of the Co–Mo–S phase the results on unsupported catalysts show that an intimate contact between cobalt and molybdenum favors formation of the Co–Mo–S phase. It is therefore likely that this may also be the case for alumina-supported catalysts. This possibility seems interesting to investigate further, especially because several previous investigators (*51, 52, 54–57*) have shown that an interaction may exist between cobalt and molybdenum in the calcined precursor state.

C. POSSIBLE STRUCTURES OF THE Co–Mo–S PHASE. COMPARISON WITH PREVIOUSLY PROPOSED MODELS

In this section the observation of a Co–Mo–S phase in sulfided catalysts and the characteristics of this phase will be compared with previously proposed structural models for HDS catalysts. Most models have been aimed at describing the structure of the industrially important alumina-supported catalysts. In Table 3 the observed characteristics for the Co–Mo–S phase are schematically compared with some of these models. The more important points will be discussed below together with the structural characteristics of unsupported catalysts.

The contact synergy model (*3, 10–12, 33*), which is based on studies of unsupported catalysts, proposes that for unsupported as well as for supported catalysts bulk phases of Co_9S_8 and MoS_2 are present. According to this model the promoting effect is associated with cobalt being present as Co_9S_8. However, this model does not account for the Co–Mo–S phase

TABLE 3

Structure of the Co–Mo–S Phase in Alumina-Supported Catalysts. Comparison with Different Models[a]

Characteristics observed for the Co–Mo–S phase	Models						
	Contact synergy model; bulk Co_9S_8 and MoS_2	Original monolayer model; Co located inside Al_2O_3	Monolayer model with Co in monolayer	Intercalation models		Single S–Mo–S slab models	
				Co intercalated in bulk of MoS_2	Co intercalated at surface of MoS_2	Co on surface	Co substituted for Mo
Co–Mo–S in unsupported catalysts	No	No	No	Yes	Yes	Yes	Yes
Cobalt in sulfur surroundings	Yes	No	No	Yes	Yes	Yes	Yes
Cobalt in a Mo-containing phase	No	No	Yes	Yes	Yes	Yes	Yes
Co atoms exposed in Al_2O_3-supported catalysts	No	No	Yes	—	Yes	Yes	Yes
Co atoms not exposed in unsupported catalysts	Yes	—	—	Yes	No	No	Yes
Reversible oxidation–reduction of Co by changing p_{H_2S}/p_{H_2}	No	Yes	Yes	Yes	Yes	Yes	Yes
Large amounts of Co in the Co–Mo–S phase	—	No	Yes	Yes	Yes	Yes	Yes
Low Debye temperature	No	No	Yes	Yes	Yes	Yes	Yes
Co–Mo–S can be regenerated	—	No	Yes	Yes	Yes	Yes	Yes
"Monolayer" dispersion of Co–Mo–S for Al_2O_3-supported catalysts (*54*)	No	No	Yes	No	No	Yes	Yes

[a] In the table, the observed characteristics are considered separately when compared with each of the models. Thus, "Yes" means that the specific observed characteristic *might* be consistent with the model, whereas "No" means lack of consistency.

observed in the present study both in alumina-supported and unsupported catalysts. Moreover, Co_9S_8 was not observed in the present Co–Mo/Al_2O_3 catalyst and the presence of Co_9S_8 is therefore not a general feature of such catalysts.

In the original monolayer model, proposed to describe the structure of alumina-supported catalysts (*1*, *5*), the cobalt atoms are assumed to be located in the support. The present results indicate that in such catalysts some of the cobalt atoms in fact remain in the alumina upon sulfiding. However, most of the cobalt atoms are found in the Co–Mo–S surface phase. Although it cannot be excluded that the fraction of cobalt atoms located in the alumina has some influence on the surface structures, as suggested in the monolayer model, the large amount of Co found in the Co–Mo–S phase is not accounted for in the original monolayer model.

Mitchell and Trifirò (*57*) have suggested a model for alumina-supported catalysts (also included in Table 3), which in some respects resembles the monolayer model. They assume that both cobalt and molybdenum, bridged to each other via oxygen or sulfur, are present at the surface of the support and that both atoms are partly sulfided and bonded via oxygen ions to the alumina. This model is consistent with many of the present observations. However, the structure proposed in the model is expected to be unique for a supported catalyst. Therefore this model is not in accordance with the presently observed similarity between supported and unsupported catalysts. Also, the present results suggest that cobalt is not bonded to oxygen ions.

In the original intercalation model (*7*), which was based on studies of unsupported Ni/WS_2 catalysts, it was assumed that Ni atoms are intercalated in the bulk WS_2 phase. By analogy it has been proposed that this model holds also for Co–Mo catalysts. MoS_2 crystallizes in a layer structure consisting of slabs made up of a Mo layer with a sulfur layer on each side. The slabs are held together by relatively weak van der Waals forces. Each of the Mo atoms is surrounded by six sulfur atoms in a trigonal prismatic coordination. It has been reported (see, e.g., Ref. (*58*)) that intercalation with alkali metal atoms such as K, Na, Li, and Cs into the MoS_2 structure (i.e., in the van der Waals gaps between the S–Mo–S slabs) can take place. However, this situation is not favorable for 3*d* metals, as theoretically predicted by Huisman *et al.* (*59*). Farragher and Cossee (*8*) proposed a model in which the 3*d*-metal atoms are assumed to enter pseudointercalation sites at the surface of small WS_2 (or MoS_2) crystals. The authors observed that about 0.02 Ni atoms per W atom could be accommodated in 50-nm-large WS_2 crystals. This number was found to correspond to the number of "atypical" sites in the lattice. With decreasing WS_2 (MoS_2) crystal size the fraction of such sites should increase and for small WS_2 (MoS_2) crystals the fraction may be as large as 0.3–1.0 (*8*). As indicated in Table 3 the intercalation models are able to explain most of the observed features of the Co–Mo–S phase, but a few observations are not easy to bring into agreement with these models. First of all it is observed that exposure of the unsupported Co/MoS_2(ppm) and Co/MoS_2(0.25) catalysts to air does not give rise to any changes in the Mössbauer spectra. This suggests that the Co–Mo–S phase does not resemble MoS_2 with cobalt atoms situated in pseudointercalation sites at the surface. Secondly, the results of a recent ir study (*54*) of Co–Mo/Al_2O_3 catalysts before and after sulfiding show, in agreement with the MES results, that the degree of dispersion of the active phases is very high in the sulfided state. In fact, the ir results suggest that the active phases cover the alumina surface to a similar extent in the calcined and in the sulfided states. This finding is not consistent with the intercalation models, which require the molybdenum monolayer, present in calcined catalysts, to be broken up during sulfiding, because at least two S–Mo–S slabs on top of each other are required in order to have intercalation or pseudointercalation sites.

In view of the difficulty of explaining all the observed characteristics of the Co–Mo–S phase in both unsupported and alumina-supported Co–Mo catalysts in terms of previously proposed structural models, an alternative description will be considered below. It is proposed that the highly dispersed Co–Mo–S phase in the Al_2O_3-supported catalyst consists of cobalt associated with small patches of single S–Mo–S slabs dispersed over the alumina surface. Since the S–Mo–S slabs are the building blocks of bulk MoS_2, the single-slab structure is in many respects MoS_2-like. It should be noted that intercalation sites do not exist in the single-slab structure. It is further proposed that as the degree of dispersion of the Co–Mo–S phase decreases multiple S–Mo–S slabs are formed (i.e., bulk MoS_2-like structures). Such three-dimensional structures correspond to the Co–Mo–S phase observed in the unsupported catalysts and presumably also in supported catalysts exhibiting weak support interactions (e.g., silica or carbon). The present results indicate that the single-slab structure is quite stable on the alumina-supported catalyst since it is found after several days of sulfiding or HDS reaction. But it is possible that upon severe aging the degree of dispersion of the Co–Mo–S phase may decrease. The relatively high stability of the single-slab structure may be related to the small difference in lattice energy between a single S–Mo–S slab and bulk MoS_2 (*60*). It is possible that the initial formation of the Co–Mo–S single-slab structure in alumina-supported catalysts and the observed ease of regeneration of this phase by calcination and resulfiding (*16*) may be related to the resemblance between the monolayer structure present in the calcined catalyst and the single-slab Co–Mo–S phase.

Different positions of Co in the S–Mo–S slabs are possible. One location will be in substitution for Mo inside or at the edges of the slabs. Another possible location could be that of individual sulfided cobalt atoms (or groups of atoms) on the surface of the slabs. Both possibilities are included in Table 3. The observation that the cobalt atoms in the Co–Mo–S phase of the unsupported catalyst are not affected by air exposure suggests that the cobalt atoms may be located at sites well below the surface and this result favors the substitutional location.

D. DEPENDENCE ON p_{H_2}/p_{H_2S}; POSSIBLE HYDRODESULFURIZATION REACTION MECHANISM

Several observations presented here and in Ref. (*25*) show that catalytic activity is associated with the Co–Mo–S surface phase. Some possibilities for the promoting role of cobalt are discussed below in view of the structure of the Co–Mo–S phase.

The mechanism for the hydrodesulfurization reaction is generally believed to require an anion vacancy where the S-containing molecule can be adsorbed via the S heteroatom, as proposed by Lipsch and Schuit (*5*). In MoS_2 (and WS_2) such an anion vacancy can be created according to the reaction

$$2Mo^{4+} + S^{2-} + H_2 \rightarrow 2Mo^{3+} + \square + H_2S \quad (3)$$

resulting in the formation of Mo^{3+} (W^{3+}). Evidence for the presence of this valence state has been found by ESR studies of Voorhoeve (*61*) and Konings *et al.* (*20*).

In Co–Mo catalysts the formation of anion vacancies may also be associated with the presence of cobalt. In Section V.C it was discussed that the cobalt atoms in the Co–Mo–S phase may substitute for molybdenum atoms in the S–Mo–S slabs. Such a substitution will most likely lead to the creation of anion vacancies. The cobalt promoter atoms may in this way increase the number of vacancies and thereby the catalytic activity of the whole structure.

Earlier MES results for supported catalysts (*16*) indicated that the Co atoms in the Co–Mo–S phase are sensitive to changes in the gaseous environment. It was observed that alternating exposure to H_2/H_2S and H_2 gave rise to a reversible reduction–oxidation of the low-spin Fe^{3+} ions, produced by the decay of ^{57}Co in the Co–Mo–S phase and this behavior can be expressed as

$$2Fe^{3+} + S^{2-} + H_2 \rightleftarrows 2Fe^{2+} + \square + H_2S. \quad (4)$$

Spectra obtained with a catalyst alternatingly exposed to H_2/thiophene and H_2 gave similar results. Although the Mössbauer results give information only on the valence state of iron atoms produced by the decay of ^{57}Co atoms in the catalyst, the chemical similarity of iron and cobalt, as well as the similarity of $Fe–Mo/Al_2O_3$ and $Co–Mo/Al_2O_3$ catalysts (*23*), suggests that such valence changes also take place for the cobalt atoms. These Mössbauer results thus indicate that another possible role of the promoter atoms may be to participate directly in the catalytic reaction.

In view of the present results on the state of Co and those obtained by other investigators on Mo, the following reaction sequence may take place. HSR is here assumed to represent the S-containing compound.

$$Mo^{4+} + Co^{2+} + \square + S^{2-} + HSR \rightarrow Mo^{3+} + Co^{3+} + SH^- + SR^-, \quad (5)$$

$$Mo^{3+} + Co^{3+} + SH^- + SR^- + H_2 \rightarrow Mo^{3+} + Co^{3+} + 2SH^- + HR\uparrow, \quad (6)$$

$$Mo^{3+} + Co^{3+} + 2SH^- \rightarrow Mo^{4+} + Co^{2+} + \square + S^{2-} + H_2S\uparrow. \quad (7)$$

The scheme and its structure implications may be visualized as shown below. In this scheme the location of cobalt is assumed to be substitutional for molybdenum in or at the edge of the S–Mo–S slab.

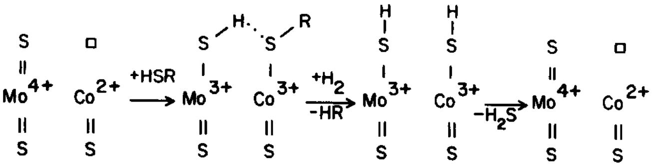

(8)

The hydrogen needed for the reaction may be supplied by adjacent -SH groups. The example above only describes the reaction on a site associated with a Co atom. However, it must be borne in mind that the reaction also takes place on sites which are not associated with Co atoms as in the case of unpromoted catalysts.

VI. CONCLUSION

The present investigation has given information about the location of cobalt in sulfided Co–Mo catalysts. The presence of a Co–Mo–S phase, which contains Co, Mo, and S in a MoS_2-like structure is revealed. The Mössbauer results suggest that Co is located in Mo sites of the structure (i.e., the composition may be represented by $Co_xMo_{1-x}S_{2\pm\delta}$). In addition it is concluded that in alumina-supported catalysts the Co–Mo–S phase has a single-slab structure. The observation of the Co–Mo–S phase in both unsupported and alumina-supported catalysts indicates that the Co–Mo–S phase is probably a quite general feature of hydrodesulfurization catalysts. Furthermore, the results suggest that the Co–Mo–S phase may be responsible for the catalytic activity of such catalysts as further substantiated in the following paper.

ACKNOWLEDGMENTS

The authors would like to thank N. Topsøe and F. Massoth for helpful discussion, J. Villadsen for conducting X-ray diffraction measurements, and J. W. Hansen for help in the preparation of the Mössbauer sources. A. C. Jacobsen, B. Cooper, B. M. Moyse, and A. Nielsen are acknowledged for their continuous interest in the work.

REFERENCES

1. Schuit, G. C. A., and Gates, B. C., *AIChE J.* **19,** 417 (1973). An updated version of this article was given by Gates, B. C., Katzer, J. R., and Schuit, G. C. A., *in* "Chemistry of Catalytic Processes," Chap. 5. McGraw–Hill, New York, 1979.
2. de Beer, V. H. J., and Schuit, G. C. A., *in* "Preparation of Catalysts" (B. Delmon, P. A. Jacobs, and G. Poncelet, Eds.), p. 343. Elsevier, Amsterdam, 1976.
3. Delmon, B., *Amer. Chem. Soc. Div. Petrol. Chem. Prepr.* **22,** 503 (1977).
4. Massoth, F. E., *in* "Advances in Catalysis and Related Subjects," Vol. 27, p. 265. Academic Press, New York/London, 1978.
5. Lipsch, J. M. J. G., and Schuit, G. C. A., *J. Catal.* **15,** 179 (1969).
6. Massoth, F. E., *J. Catal.* **36,** 164 (1975).
7. Voorhoeve, R. J. H., and Stuiver, J. C. M., *J. Catal.* **23,** 243 (1971).
8. Farragher, A. L., and Cossee, P., *in* "Proceedings, 5th International Congress on Catalysis, Palm Beach, 1972" (J. W. Hightower, Ed.), p. 1301. North-Holland, Amsterdam, 1973.
9. Farragher, A. L., Symposium on the Role of Solid State Chemistry in Catalysis, ACS Meeting, New Orleans, March 20–25, 1977.
10. Hagenbach, G., Courty, P., and Delmon, B., *J. Catal.* **31,** 264 (1973).
11. Grange, P., and Delmon, B., *J. Less Common Metals* **36,** 353 (1974).
12. Hagenbach, G., Courty, P., and Delmon, B., *J. Catal.* **23,** 295 (1971).
13. Furimsky, E., and Amberg, C. H., *Can J. Chem.* **53,** 2542 (1975).
14. Wise, H., 2nd International Conference on the Chemistry and Uses of Molybdenum, Oxford, 1976.
15. Phillips, R. W., and Fote, A. A., *J. Catal.* **41,** 168 (1976).
16. Clausen, B. S., Mørup, S., Topsøe, H., and Candia, R., *J. Phys. Paris* **37,** C6-249 (1976).
17. Broderick, D. H., Schuit, G. C. A., and Gates, B. C., *J. Catal.* **54,** 94 (1978).
18. Topsøe, H., and Mørup, S. *in* "Proceedings, Int. Conf. Mössbauer Spectroscopy, Cracow, Poland, 1975" (A. Z. Hrynkiewicz and J. A. Sawicki, Eds.), Vol. 1, p. 305.
19. Clausen, B. S., M. Sc. thesis, LTF II, Technical University of Denmark, 1976.
20. Konings, A. J. A., van Dooren, A. M., Koningsberger, D. C., de Beer, V. H. J., Farragher, A. L., and Schuit, G. C. A., *J. Catal.* **59,** 1 (1978).
21. Dumesic, J. A. and Topsøe, H., *in* "Advances in Catalysis and Related Subjects," Vol. 26, p. 121. Academic Press, New York/London, 1977; Topsøe, H., Dumesic, J. A., and Mørup, S., *in* "Applications of Mössbauer Spectroscopy" (R. L. Cohen, Ed.), Vol. II, p. 55. Academic Press, New York, 1980.
22. Topsøe, H., Clausen, B. S., Burriesci, N., Candia, R., and Mørup, S., Proceedings, 2nd International Symposium on Scientific Bases for the Preparation of Heterogeneous Catalysts (Louvain-la-Neuve, 1978), Preparation of Catalysts II (B. Delmon, P. Grange, P. Jacobs, and G. Poncelet, Eds.), p. 479. Elsevier, Amsterdam/New York, 1979.
23. Mørup, S., Clausen, B. S., and Topsøe, H., *J. Phys. Paris* **40,** C2-88 (1979).
24. Clausen, B. S., Ph.D. dissertation, LTF II, Technical University of Denmark, 1979.
25. Wivel, C., Candia, R., Clausen, B. S., Mørup, S., and Topsøe, H., *J. Catal.* **68,** 453 (1981).
26. Wertheim, G. K., *Accounts Chem. Res.* **4,** 373 (1971); Friedt, J. M., and Danon, J., *Radiochim. Acta* **17,** 173 (1972); Seregin, P. P., Nasredinov, F. S., and Vasilev, L. N., *Phys. Status Solidi A* **45,** 11 (1978).
27. Wertheim, G. K., *Phys. Rev.* **124,** 764 (1961).
28. Gol'danskii, V. I., and Makarov, E. F. *in* "Chemical Applications of Mössbauer Spectroscopy" (V. I. Gol'danskii and R. H. Herber, Eds.), p. 1. Academic Press, New York, 1968.
29. McKinley, J. B. *in* "Catalysis" (P. H. Emmett, Ed.) Vol. 5, p. 405. Reinhold, New York, 1957.
30. Van den Berg, J. M., *Inorg. Chim. Acta* **2,** 216 (1968).
31. Chevrel, R., Sergent, M., and Prigent, J., *C.R. Acad. Sci. Paris* **267,** 1135 (1968).
32. Sørensen, K., Internal Report No. 1, LTF II, Technical University of Denmark, 1972.
33. Delmon, B., 3rd International Conference on the Chemistry and Uses of Molybdenum, Ann Arbor, Michigan, 1979.
34. Zabala, J. M., Mainil, M., Grange, P., and Delmon, B., *React. Kinet. Catal. Lett.* **3,** 285 (1975).
35. Lo Jacono, M., Verbeek, J. L., and Schuit, G. C. A., *J. Catal.* **29,** 463 (1973).
36. Clausen, B. S., Topsøe, H., Villadsen, J., Mørup, S., and Candia, R., *in* "Proceedings, Int. Conf. Mössbauer Spectroscopy, Bucharest, Romania, 1977" (D. Barb and D. Tarina, Eds.), Vol. 1, p. 177.
37. Lindqvist, M., Lundqvist, D., and Westgren, A., *Sv. Kem. Tidskr.* **48,** 156 (1936).
38. Townsend, M. G., Harwood, J. L., Tremblay, R. J., and Ripley, L. G., *Phys. Status Solidi A* **9,** K137 (1972).
39. Elliott, N., *J. Chem. Phys.* **33,** 903 (1960).
40. Morris, B., Johnson, V., and Wold, A., *J. Phys. Chem. Solids* **28,** 1565 (1967).
41. McCann, V. H., and Ward, J. B., *J. Phys. Chem. Solids* **38,** 991 (1977).
42. Lundqvist, D., and Westgren, A., *Z. Anorg. Allg. Chem.* **239,** 85 (1938).

43. Bouchard, R. J., Russo, P. A., and Wold, A., *Inorg. Chem.* **4,** 685 (1965).
44. Rosenqvist, T., *J. Iron Steel Inst.* **176,** 37 (1954).
45. Heidelberg, R. F., Luxem, A. H., Talhouk, S., and Banewicz, J. J., *Inorg. Chem.* **5,** 194 (1966).
46. Anzenhofer, K., and de Boer, J. J., *Acta Crystallogr. B* **25,** 1419 (1969).
47. Eibschütz, M., Lines, M. E., and Disalvo, F. J., *Phys. Rev. B* **15,** 103 (1977).
48. Ingalls, R., Van der Woude, F., and Sawatsky, G. A. *in* "Mössbauer Isomer Shifts" (G. K. Shenoy and F. E. Wagner, Eds.), North-Holland, Amsterdam, 1978.
49. Nishihara, Y., and Ogawa, S., *J. Phys. Paris* **40,** C2-297 (1979).
50. Chianelli, R. R., Prestridge, E. B., Pecoraro, T. A., and DeNeufville, J. P., *Science* **203,** 1105 (1979).
51. Richardson, J. T., *Ind. Eng. Chem. Fundam.* **3,** 154 (1964).
52. Chung, K. S., and Massoth, F. E., *J. Catal.* **64,** 320, 332 (1980).
53. Declerck-Grimee, R. I., Canesson, P., Friedman, R. M., and Fripiat, J. J., *J. Phys. Chem.* **82,** 885, 889 (1978).
54. Topsøe, N., *J. Catal.* **64,** 235 (1980).
55. Moné, R., International Conference on the Scientific Basis for the Preparation of Solid Catalysts, Brussels, D3, 1975.
56. Ratnasamy, P., and Knözinger, H., *J. Catal.* **54,** 155 (1978).
57. Mitchell, P. C. H., and Trifirò, F., *J. Catal.* **33,** 350 (1974).
58. Tsigdinos, G. A., *in* "Topics in Current Chemistry. 76. Aspects of Molybdenum and Related Chemistry." Springer Verlag, New York/Berlin, 1978.
59. Huisman, R., de Jonge, R., Haas, C., and Jellineck, F., *J. Solid State Chem.* **3,** 56 (1971).
60. Hartman, P., *Acta Crystallogr.* **11,** 365 (1958).
61. Voorhoeve, R. J. H., *J. Catal.* **23,** 236 (1971).